DESY 14-048
HU-EP-14/14
IFIC/14-24
CP3-Origins-2014-011 DNRF90
DIAS-2014-11
LPT-Orsay/14-19
MITP/14-026
MS-TP-14-18
SFB/CPP-14-20
TCD 14–03

Decay constants of B-mesons from non-perturbative HQET with two light dynamical quarks

ALPHA Collaboration

Fabio Bernardoni[a], Benoît Blossier[b], John Bulava[c], Michele Della Morte[d,e], Patrick Fritzsch[f], Nicolas Garron[c], Antoine Gérardin[b], Jochen Heitger[g], Georg von Hippel[h], Hubert Simma[a], Rainer Sommer[a]

[a] NIC @ DESY, Platanenallee 6, 15738 Zeuthen, Germany
[b] Laboratoire de Physique Théorique, Université Paris XI, 91405 Orsay Cedex, France
[c] School of Mathematics, Trinity College, Dublin 2, Ireland
[d] CP^3-Origins & Danish IAS, University of Southern Denmark, Campusvej 55, 5230 Odense M, Denmark
[e] IFIC and CSIC, Calle Catedrático José Beltran 2, 46980 Paterna, Valencia, Spain
[f] Institut für Physik, Humboldt-Universität zu Berlin, Newtonstr. 15, 12489 Berlin, Germany
[g] Institut für Theoretische Physik, Universität Münster, Wilhelm-Klemm-Str. 9, 48149 Münster, Germany
[h] PRISMA Cluster of Excellence, Institut für Kernphysik, University of Mainz, Becherweg 45, 55099 Mainz, Germany

Abstract

We present a computation of B-meson decay constants from lattice QCD simulations within the framework of Heavy Quark Effective Theory for the b-quark. The next-to-leading order corrections in the HQET expansion are included non-perturbatively. Based on $N_\mathrm{f} = 2$ gauge field ensembles, covering three lattice spacings $a \approx (0.08 - 0.05)\,\mathrm{fm}$ and pion masses down to 190 MeV, a variational method for extracting hadronic matrix elements is used to keep systematic errors under control. In addition we perform a careful autocorrelation analysis in the extrapolation to the continuum and to the physical pion mass limits. Our final results read $f_\mathrm{B} = 186(13)\,\mathrm{MeV}$, $f_{\mathrm{B_s}} = 224(14)\,\mathrm{MeV}$ and $f_{\mathrm{B_s}}/f_\mathrm{B} = 1.203(65)$. A comparison with other results in the literature does not reveal a dependence on the number of dynamical quarks, and effects from truncating HQET appear to be negligible.

Keywords: Lattice QCD, Heavy Quark Effective Theory, Bottom quarks, Meson decay
PACS: 12.38.Gc, 12.39.Hg, 14.65.Fy, 13.20.-v

1 Introduction

In the ongoing quest for new effects in high-energy particle physics, flavour physics provides information complementary to that from the direct searches performed at ATLAS and CMS. Indeed, low-energy processes and rare events can be sensitive probes of New Physics, in particular when they are mediated by virtual loops, in which non-Standard Model particles can circulate, or when they involve new couplings occurring at tree-level. However, any analysis of experimental data in the quark sector depends on theoretical inputs, such as hadron decay constants, that encode the long-distance dynamics of QCD, which cannot be reliably estimated in perturbation theory.

In this regard, B-physics is an emblematic case. For example, it is crucial to understand the origin of the current discrepancy in the Cabibbo–Kobayashi–Maskawa matrix element $V_{\rm ub}$ measured through the exclusive processes $B \to \tau\nu$ [1, 2] and $B \to \pi\ell\nu$ [3, 4], where the latter makes use of the $B \to \pi$ form factors computed on the lattice. Is it due to an experimental problem, or due to new physics such as the presence of a new, right-handed, tree-level coupling to a charged Higgs boson in the B leptonic decay [5], or due to a severe underestimate of the uncertainty on the decay constant $f_{\rm B}$ governing that decay. For comparison, the recent measurements of $\mathcal{B}(B_{\rm s} \to \mu^+\mu^-)$ at LHC [6, 7] are in excellent agreement with the Standard Model prediction [8,9], where the latter depends on the decay constant $f_{\rm B_s}$, whose estimate is dominated by lattice results.

The methods that have been used to estimate $f_{\rm B}$ and $f_{\rm B_s}$ include applications of quark models, as discussed in [10–12] and references therein, and QCD sum rules in the analysis of two-point B-meson correlators [13–16]. Several strategies have been proposed to determine $f_{\rm B}$ and $f_{\rm B_s}$ from first principles using lattice field theory, including the extrapolation of simulation results obtained in the region between the charm quark mass $m_{\rm c}$ and a mass $\sim 3m_{\rm c}$ to the physical b-quark mass $m_{\rm b}$ [17,18], simulations of relativistic b-quarks using an action tuned so as to minimize discretization errors [19,20], and the use of Non-Relativistic QCD [21, 22]. We here use Heavy Quark Effective Theory (HQET) [23–26], regularized on the lattice with the parameters of HQET determined by a non-perturbative matching to QCD [27–29]. The virtue of this approach is that perturbative errors are absent and the continuum limit exists. The matching at order $\mathrm{O}(1/m_{\rm h})$ has been performed in the $N_{\rm f} = 2$ theory [30]; this is the first step required, for example, in order to compute the b-quark mass [31], which we use in this letter to extract $f_{\rm B}$, $f_{\rm B_s}$ and $f_{\rm B_s}/f_{\rm B}$ from our simulations. In Section 2, we review the methods employed, before presenting the results in Section 3. Section 4 contains our conclusions.

2 Methodology

2.1 HQET on the lattice

Heavy Quark Effective Theory regularized on the lattice is a well-defined approach to B-physics. It is based on an expansion in powers of $1/m_{\rm h}$ of QCD correlation functions around the limit $1/m_{\rm h} \to 0$. The continuum limit can be taken order by order in the expansion, since it only requires correlation functions computed in the static theory, which is non-perturbatively renormalizable. Applying the strategy previously discussed in [27, 29, 32] and employed to measure $f_{\rm B_s}$ in the quenched approximation [33], the HQET action and

	$\beta = 5.5$		$\beta = 5.3$		$\beta = 5.2$	
	HYP1	HYP2	HYP1	HYP2	HYP1	HYP2
$am_{\rm bare}^{\rm stat}$	0.969(10)	1.000(10)	1.317(13)	1.350(13)	1.520(15)	1.554(15)
$-\ln(Z_{\rm A}^{\rm stat})$	0.271(5)	0.181(5)	0.283(5)	0.177(5)	0.291(6)	0.177(6)
$am_{\rm bare}$	0.594(16)	0.606(16)	0.993(18)	1.014(18)	1.214(19)	1.239(19)
$-\ln(Z_{\rm A}^{\rm HQET})$	0.156(42)	0.163(36)	0.169(37)	0.146(32)	0.169(35)	0.136(31)
$-c_{\rm A}^{\rm HQET}/a$	0.07(12)	0.67(12)	0.00(10)	0.55(10)	0.01(9)	0.54(9)
$\omega_{\rm kin}/a$	0.520(13)	0.525(13)	0.415(10)	0.419(10)	0.378(9)	0.380(9)
$\omega_{\rm spin}/a$	0.949(40)	1.090(46)	0.731(31)	0.883(37)	0.655(27)	0.812(33)

Table 1: HQET parameters at the physical point $\boldsymbol{\omega}(z = z_{\rm b})$. The parameters are given for $z_{\rm b}$ determined such that $m_{\rm B} = 5279.5\,\mathrm{MeV}$ [31], which corresponds to $z_{\rm b}^{\rm stat} = 13.24(25)$ at static order, and to $z_{\rm b} = 13.25(26)$ for HQET expanded to $\mathrm{O}(1/m_{\rm h})$. The bare coupling is $g_0^2 = 6/\beta$.

the time component of the axial current expanded to $\mathrm{O}(1/m_{\rm h})$ read

$$S_{\rm HQET} = a^4 \sum\nolimits_x \left\{ \mathscr{L}_{\rm stat}(x) - \omega_{\rm kin}\mathcal{O}_{\rm kin}(x) - \omega_{\rm spin}\mathcal{O}_{\rm spin}(x) \right\}, \tag{2.1}$$

$$\mathscr{L}_{\rm stat}(x) = \overline{\psi}_{\rm h}(x)\, D_0\, \psi_{\rm h}(x)\,, \tag{2.2}$$

$$\mathcal{O}_{\rm kin}(x) = \overline{\psi}_{\rm h}(x)\, \mathbf{D}^2\, \psi_{\rm h}(x)\,, \tag{2.3}$$

$$\mathcal{O}_{\rm spin}(x) = \overline{\psi}_{\rm h}(x)\, \boldsymbol{\sigma}\cdot\mathbf{B}\, \psi_{\rm h}(x)\,, \tag{2.4}$$

and

$$A_0^{\rm HQET}(x) = Z_{\rm A}^{\rm HQET}\Big[A_0^{\rm stat}(x) + \sum\nolimits_{i=1}^{2} c_{\rm A}^{(i)} A_0^{(i)}(x)\Big]\,, \tag{2.5}$$

$$A_0^{(1)}(x) = \overline{\psi}_q\, \tfrac{1}{2}\gamma_5\gamma_i(\nabla_i^{\rm S} - \overleftarrow{\nabla}_i^{\rm S})\, \psi_{\rm h}(x)\,, \tag{2.6}$$

$$A_0^{(2)}(x) = \overline{\psi}_q\, \tfrac{1}{2}\gamma_5\gamma_i(\nabla_i^{\rm S} + \overleftarrow{\nabla}_i^{\rm S})\, \psi_{\rm h}(x)\,, \quad A_i^{\rm stat}(x) = \overline{\psi}_q(x)\, \gamma_i\gamma_5\, \psi_{\rm h}(x)\,. \tag{2.7}$$

We use the labels h to denote the heavy (static) quark field appearing in the HQET Lagrangian, and $q = \mathrm{u/d, s}$ for the light and strange quark channels, respectively. The normalization is such that the classical values of the coefficients are $\omega_{\rm kin} = \omega_{\rm spin} = -c_{\rm A}^{(i)} = 1/(2m_{\rm h})$. A bare mass $m_{\rm bare}$ has to be added to the energy levels computed with this Lagrangian in order to obtain the QCD ones. At the classical level it is $m_{\rm h}$, but in the quantized theory, it has to further compensate a power divergence. The heavy quark field $\psi_{\rm h}$ obeys $\frac{1+\gamma_0}{2}\psi_{\rm h} = \psi_{\rm h}$, and all spatial derivatives are symmetrized:

$$\tilde{\partial}_i = \tfrac{1}{2}(\partial_i + \partial_i^*)\,, \qquad \nabla_i^{\rm S} = \tfrac{1}{2}(\nabla_i + \nabla_i^*)\,, \qquad \overleftarrow{\nabla}_i^{\rm S} = \tfrac{1}{2}(\overleftarrow{\nabla}_i + \overleftarrow{\nabla}_i^*)\,. \tag{2.8}$$

In QCD the decay constant $f_{\rm B_q}$ is given by $\langle 0|\bar{q}\gamma_0\gamma_5 b|B_q(\mathbf{p}=0)\rangle = f_{\rm B_q} m_{\rm B_q}$, with the relativistic convention $\langle B_q(\mathbf{p}')|B_q(\mathbf{p})\rangle = 2E_q(p)\delta(\mathbf{p}-\mathbf{p}')$. We are thus interested in extracting matrix elements from correlation functions defined at zero spatial momentum; the operator $A_0^{(2)}$ therefore does not enter into our present computations at all.

In order to assure the renormalizability of HQET at next-to-leading order, the $\mathrm{O}(1/m_{\rm h})$ terms in (2.1) are treated in the usual way as operator insertions into static correlation

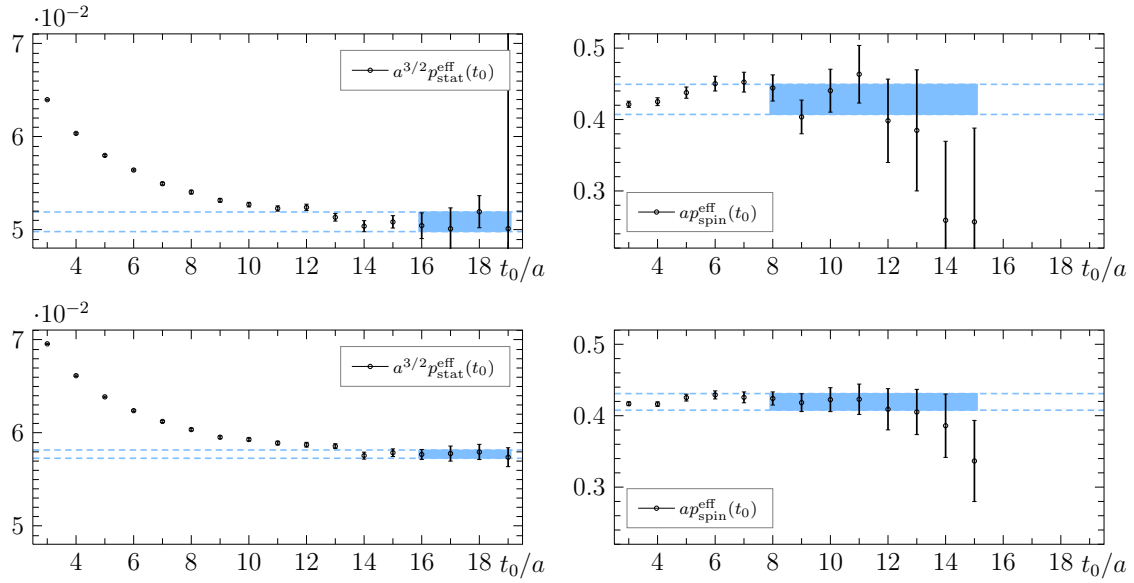

Figure 1: Typical plateau averages after applying the GEVP analysis to data obtained on the $N_{\rm f} = 2$ CLS ensemble N6 ($a = 0.048\,$fm, $m_\pi = 340\,$MeV). The two plots on top show our result for the B-meson static matrix element $p^{\rm stat}$ (left panel) and the $\mathrm{O}(1/m_{\rm h})$ chromomagnetic matrix element $p^{\rm spin}$ (right panel). In the lower plots we present the corresponding quantities for the $\mathrm{B_s}$-meson.

functions,

$$\langle O \rangle = \langle O \rangle_{\rm stat} + \omega_{\rm kin}\, a^4 \sum\nolimits_x \langle O\, \mathcal{O}_{\rm kin}(x) \rangle_{\rm stat} + \omega_{\rm spin}\, a^4 \sum\nolimits_x \langle O\, \mathcal{O}_{\rm spin}(x) \rangle_{\rm stat}\ , \tag{2.9}$$

where the suffix "stat" reminds us that expectation values are computed in the static theory.

In our strategy we can treat HQET non-perturbatively to leading order (static) or next-to-leading order, including terms of $\mathrm{O}(1/m_{\rm h})$. The corresponding sets of parameters, $\boldsymbol{\omega}^{\rm stat} \equiv \left(m^{\rm stat}_{\rm bare}, Z^{\rm stat}_{\rm A}\right)$ or $\boldsymbol{\omega} \equiv \left(m_{\rm bare}, \omega_{\rm kin}, \omega_{\rm spin}, Z^{\rm HQET}_{\rm A}, c^{(1)}_{\rm A}\right)$ absorb power and logarithmic divergences of the effective theory regularized on the lattice. For technical reasons they have been determined in [30] for a series of heavy quark masses parameterized in terms of the renormalization group invariant (RGI) heavy quark mass $z \equiv ML_1$.[1] After our recent determination of the RGI b-quark mass $z_{\rm b} \equiv M_{\rm b} L_1$ [31], we now choose a quadratic polynomial to interpolate $\boldsymbol{\omega}(z)$ — computed at $z = 11, 13, 15$ — to the physical point $z_{\rm b} = 13.25$. Similarly, we interpolate $\boldsymbol{\omega}^{\rm stat}(z)$ to $z^{\rm stat}_{\rm b} = 13.24$ at the static order. As expected from [30], all individual interpolations of the $\boldsymbol{\omega}^{(\rm stat)}(z)$ parameters to $z^{(\rm stat)}_{\rm b}$ are smooth and do not deviate much from the closest point at $z = 13$. In the following we will refer to the HQET parameters at the physical b-quark mass only. For completeness they are collected in Table 1 for the three lattice spacings $a(\beta)$ and two static discretizations (HYP1, HYP2) in use.

2.2 Isolating the ground state

In extracting hadronic quantities, it is crucial to have good control over the contributions of excited states to the correlators. Since we are interested in the lowest-lying state in a given

[1] The length scale L_1 is implicitly defined through the renormalized coupling in the Schrödinger Functional scheme $\bar{g}^2_{\rm SF}(L_1/2) = 2.989$, see [30, 34].

channel, we attempt to suppress excited-state contaminations by considering appropriate linear combinations of correlation functions. Specifically, we form the matrices

$$\begin{aligned} C_{ij}^{\rm stat}(t) &= \sum_{x,\mathbf{y}} \left\langle O_i(x_0+t,\mathbf{y})\, O_j^*(x)\right\rangle_{\rm stat} , \\ C_{ij}^{\rm kin/spin}(t) &= \sum_{x,\mathbf{y},z} \left\langle O_i(x_0+t,\mathbf{y})\, \mathcal{O}_{\rm kin/spin}(z)\, O_j^*(x)\right\rangle_{\rm stat} , \end{aligned} \tag{2.10}$$

which depend on a basis of operators O_i , $i = 1, \ldots, N$. The key step is to find a solution to the generalized eigenvalue problem (GEVP) in the static approximation

$$C^{\rm stat}(t)\, v_n^{\rm stat}(t,t_0) = \lambda_n^{\rm stat}(t,t_0)\, C^{\rm stat}(t_0)\, v_n^{\rm stat}(t,t_0) , \quad n = 1, \ldots, N , \quad t > t_0 . \tag{2.11}$$

Then, exploiting the orthogonality property of the eigenvectors,

$$\langle v_m^{\rm stat}(t,t_0) C^{\rm stat}(t_0) v_n^{\rm stat}(t,t_0)\rangle \propto \delta_{nm} ,$$

one can show that the $\mathrm{O}(1/m_{\rm h})$ corrections to the matrix elements $\langle 0|\overline{\psi}_{\rm h}\gamma_0\gamma_5\psi_q|B^{(n)}\rangle$ only depend on the static generalized eigenvalues $\lambda_n^{\rm stat}(t,t_0)$, the vectors $v_n^{\rm stat}(t,t_0)$, and the $\mathrm{O}(1/m_{\rm h})$ correlators $C^{\rm kin/spin}(t)$ [35], in analogy with perturbation theory in quantum mechanics.

We define the operator basis

$$O_k(x) = \overline{\psi}_{\rm h}(x)\,\gamma_0\gamma_5\,\psi_q^{(k)}(x) , \qquad \psi_q^{(k)}(x) = \left(1+\kappa_{\rm G}\, a^2\,\Delta\right)^{R_k}\psi_q(x) , \tag{2.12}$$

where $\psi_{\rm h}(x)$ is the static quark field and $\psi_q^{(k)}(x)$ ($q = \mathrm{u/d}$ or $q = \mathrm{s}$) is a Gaussian smeared [36] relativistic quark field. The gauge links in the covariant Laplacian Δ have been triply APE smeared [37, 38] in the spatial directions.

The parameters $\kappa_{\rm G}$ and R_k have been chosen such that they correspond to approximately the same sequence of physical radii at each value of the lattice spacing, see [31] for details. We solve the GEVP for the matrix of correlators in the static limit, eq. (2.11) for $N = 3$. The resulting eigenvalues and eigenvectors, together with the matrices in eq. (2.10) and the correlators

$$C_{A_0,j}^{\rm stat/(1)}(t) = \sum_{x,\mathbf{y}} \left\langle A_0^{\rm stat/(1)}(x_0+t,\mathbf{y}) O_j^*(x)\right\rangle_{\rm stat} , \tag{2.13}$$

are used to build optimal interpolating fields such that the matrix elements $\langle 0|A_0^{\rm stat}|B^{(n)}\rangle$ and their $\mathrm{O}(1/m_{\rm h})$ corrections can be extracted, from the correlation functions above, up to contaminations from excited states which are $\mathrm{O}(e^{-(E_{N+1}^{\rm stat}-E_n^{\rm stat})t_0})$. Notice that for the ground state the energy difference in the exponential correction is of the form $E_{N+1} - E_1$ rather than $E_2 - E_1$, with N the rank of the correlator matrices in eq. (2.10). This asymptotic convergence holds for $t_0 \geq t/2$, as discussed in detail in [35], to which we refer for any unexplained notation. In particular, the symbols $p^{\rm stat/x/A^{(1)}} = p_{n=1}^{\rm stat/x/A^{(1)}}$, with x=kin/spin, are used in the following to indicate the static and $\mathrm{O}(1/m_{\rm h})$ contributions to the matrix elements of the axial current as in [33], where one can find expressions for the expected time dependence of the different terms, which read

$$\begin{aligned} p_n^{\rm eff,\,stat}(t,t_0) &= p_n^{\rm stat} + \gamma_{n,N}^{\rm stat} e^{-(E_{N+1}^{\rm stat}-E_n^{\rm stat})t_0} , \\ p_n^{\rm eff,\,x}(t,t_0) &= p_n^{\rm x} + \left[\gamma_{n,N}^{\rm x} - \frac{\gamma_{n,N}^{\rm stat}}{p_n^{\rm stat}} t_0 (E_{N+1}^{\rm x} - E_n^{\rm x})\right] e^{-(E_{N+1}^{\rm stat}-E_n^{\rm stat})t_0} , \\ p_n^{\rm eff,\,A^{(1)}}(t,t_0) &= p_n^{\rm A^{(1)}} + \gamma_{n,N}^{\rm A^{(1)}}\, e^{-(E_{N+1}^{\rm stat}-E_n^{\rm stat})t_0} . \end{aligned} \tag{2.14}$$

		$f_{\rm B}$ [MeV]		$f_{\rm B_s}$ [MeV]		$f_{\rm B_s}/f_{\rm B}$	
e-id	y	HYP1	HYP2	HYP1	HYP2	HYP1	HYP2
A4	0.0771(14)	212(9)	210(10)	227(8)	227(8)	1.071(28)	1.084(23)
A5	0.0624(13)	206(7)	204(7)	226(6)	224(6)	1.096(20)	1.100(19)
B6	0.0484(9)	198(8)	195(7)	224(8)	223(7)	1.127(36)	1.144(32)
E5	0.0926(15)	215(7)	213(8)	232(8)	231(9)	1.077(28)	1.086(25)
F6	0.0562(9)	203(8)	201(8)	228(7)	228(7)	1.120(48)	1.138(39)
F7	0.0449(7)	201(6)	200(6)	222(6)	223(7)	1.103(26)	1.119(24)
G8	0.0260(5)	190(8)	190(8)	–	–	–	–
N5	0.0940(24)	222(16)	221(15)	–	–	–	–
N6	0.0662(10)	205(14)	205(15)	229(15)	231(15)	1.115(50)	1.126(46)
O7	0.0447(7)	199(14)	194(14)	–	228(14)	–	1.178(85)
LO	$y^{\rm exp}, a = 0$	188(12)		225(13)		1.184(60)	
NLO	$y^{\rm exp}, a = 0$	186(12)		–		1.203(61)	

Table 2: Raw data for $f_{\rm B}$, $f_{\rm B_s}$ and their ratio $f_{\rm B_s}/f_{\rm B}$, using HQET parameters at the physical point $\boldsymbol{\omega}(z = z_{\rm b})$, with $z_{\rm b} = 13.25$ as determined in [31]. The last two rows summarize our results of a combined chiral and continuum extrapolation using either the LO or the NLO fit ansatz (3.1) for each individual observable.

We provide in Figure 1 an illustration of typical plateaux for the heavy-light and heavy-strange mesons matrix elements $p^{\rm stat}$ and $p^{\rm spin}$. Those plateaux are chosen following the procedure detailed in [33, 39]. The criteria use the results of the GEVP analysis to ensure that in the plateau region the systematic errors due to excited-state contributions are less than a given fraction (typically one third) of the statistical errors. As a consistency check, we have also employed a global fit of the form of eqs. (2.14) to our data. The values of p_n obtained from the fit were consistent with the plateau values, albeit with smaller statistical errors. Our errors may therefore be seen as a conservative estimate.

2.3 B-meson decay constants at different orders in HQET

The quantities of interest are obtained by combining the lattice parameters of HQET, computed non-perturbatively, and the bare matrix elements evaluated in the static theory. All divergences of the effective quantum field theory are thus properly removed and the continuum limit can be safely taken at a fixed order in the $1/m_{\rm h}$ expansion.

To obtain $f_{\rm B}$ and $f_{\rm B_s}$ including $\mathrm{O}(1/m_{\rm h})$ terms in HQET, we compute

$$\phi_i = \ln(Z_{\rm A}^{\rm HQET}) + b_{\rm A}^{\rm stat} a m_{{\rm q},i} + \left(\ln(a^{3/2} p^{\rm stat}) + \omega_{\rm kin}\, p^{\rm kin} + \omega_{\rm spin}\, p^{\rm spin} + c_{\rm A}^{(1)}\, p^{{\rm A}_0^{(1)}}\right)\Big|_{m_{{\rm q},i}},$$
$$f_{{\rm B}_i} = \exp(\phi_i)/\sqrt{a^3\, m_{{\rm B}_i}/2}\,. \tag{2.15}$$

Here, i labels the light quark content (u/d- or s-quark) and the term multiplying $b_{\rm A}^{\rm stat}$ is needed for the $\mathrm{O}(a)$ improvement of mass-dependent cutoff effects in the heavy-light axial

		$f_{\rm B}^{\rm stat}$ [MeV]		$f_{\rm B_s}^{\rm stat}$ [MeV]		$f_{\rm B_s}^{\rm stat}/f_{\rm B}^{\rm stat}$	
e-id	y	HYP1	HYP2	HYP1	HYP2	HYP1	HYP2
A4	0.0771(14)	240(4)	228(4)	264(5)	250(4)	1.101(9)	1.096(7)
A5	0.0624(13)	235(4)	223(4)	265(5)	249(4)	1.128(6)	1.117(5)
B6	0.0484(9)	224(5)	213(4)	259(4)	244(4)	1.154(20)	1.143(15)
E5	0.0926(15)	240(4)	231(4)	263(4)	252(4)	1.092(10)	1.090(8)
F6	0.0562(9)	224(5)	214(4)	257(4)	245(4)	1.149(18)	1.148(16)
F7	0.0449(7)	219(4)	210(3)	252(4)	241(4)	1.152(10)	1.144(10)
G8	0.0260(5)	212(4)	205(4)	–	–	–	–
N5	0.0940(24)	241(6)	236(6)	–	–	–	–
N6	0.0662(10)	225(7)	217(5)	254(4)	245(4)	1.129(24)	1.133(18)
O7	0.0447(7)	217(9)	208(7)	–	244(6)	–	1.172(39)
LO	$y^{\rm exp}, a = 0$	192.5(52)		234.1(48)		1.219(25)	
NLO	$y^{\rm exp}, a = 0$	190.3(51)		–		1.189(24)	

Table 3: Raw data for $f_{\rm B}^{\rm stat}$, $f_{\rm B_s}^{\rm stat}$ and their ratio $f_{\rm B_s}^{\rm stat}/f_{\rm B}^{\rm stat}$, using static HQET parameters at the physical point $\boldsymbol{\omega}^{\rm stat}(z = z_{\rm b}^{\rm stat})$, with $z_{\rm b}^{\rm stat} = 13.24$ as determined in [31]. The last two rows summarize our results for a combined chiral and continuum extrapolation using either the LO or NLO fit ansatz (3.1) for each individual observable.

current.[2] The corresponding expression in static HQET is given by

$$\begin{aligned} \phi_i^{\rm stat} &= \ln(Z_{\rm A}^{\rm stat}) + b_{\rm A}^{\rm stat} a m_{{\rm q},i} + \left(\ln(a^{3/2} p^{\rm stat}) + a c_{\rm A}^{\rm stat} p^{{\rm A}_0^{(1)}}\right)\Big|_{m_{{\rm q},i}}, \\ f_{{\rm B}_i}^{\rm stat} &= \exp\{\phi_i^{\rm stat}\}/\sqrt{a^3\, m_{{\rm B}_i}/2}\,, \end{aligned} \tag{2.16}$$

where $c_{\rm A}^{\rm stat}$ is another O(a) improvement coefficient that is needed at the static order. Both $b_{\rm A}^{\rm stat}$ and $c_{\rm A}^{\rm stat}$ have been computed perturbatively in [40]. If treated as an independent observable, the ratio $f_{\rm B_s}/f_{\rm B}$ is easily obtained through eq. (2.15) at next-to-leading order, *viz.*

$$f_{\rm B_s}/f_{\rm B} = \exp\{\phi_{\rm s} - \phi\}/\sqrt{m_{\rm B_s}/m_{\rm B}}\,, \tag{2.17}$$

or in the very same way through eq. (2.16) at the static order. Note that in the ratio the leading dependence on the scale setting procedure, which explicitly enters via the lattice spacing appearing as $a^{3/2}$, cancels. Furthermore, terms in eq. (2.15) or eq. (2.16), which do not carry an explicit label i drop out and the term multiplying $b_{\rm A}^{\rm stat}$ becomes independent of the critical hopping parameter $\kappa_{\rm crit}(g_0^2)$.

Concerning the parameters and overall statistics of the large-volume simulations used in the present analysis we refer the reader to Table 1 of [31]. The light quark is treated in a unitary setup with m_π covering a range from 190 MeV to 440 MeV while the bare strange quark mass is tuned on each CLS ensemble using the kaon decay constant [34]. The lattice spacings are $a/{\rm fm} \in \{0.048, 0.065, 0.075\}$ for $\beta \in \{5.5, 5.3, 5.2\}$, corresponding to the CLS ensemble ids N-O, E-G and A-B respectively. In Table 2 we give our results for $f_{\rm B}$, $f_{\rm B_s}$ and $f_{\rm B_s}/f_{\rm B}$ as computed on these ensembles together with the results obtained after performing

[2] The bare mass $a m_{{\rm q},i} = (1/\kappa_i - 1/\kappa_{\rm crit})/2$ is obtained from $\kappa_{\rm crit}$, the point where the PCAC mass vanishes.

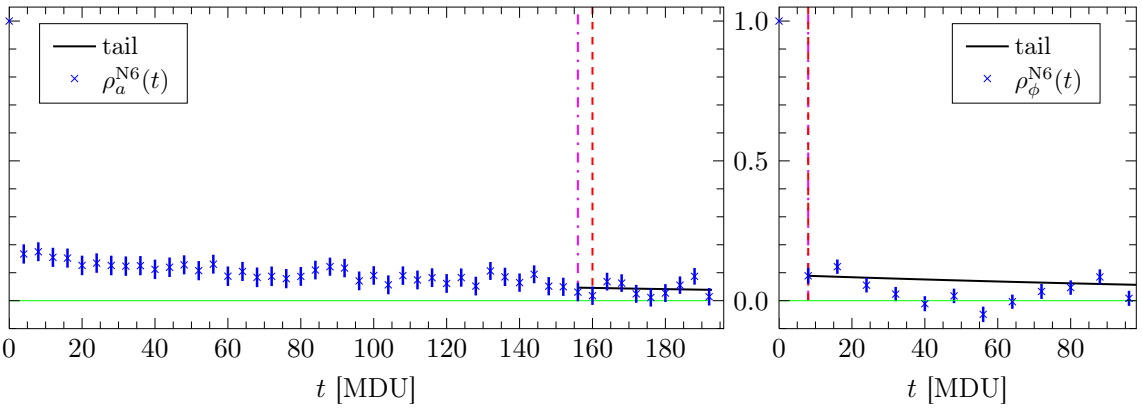

Figure 2: Example of long-tail contributions to the total budget from ensemble N6 ($\tau_{\mathrm{exp}}^{\mathrm{N6}} = 200\,\mathrm{MDU}$). On the left we plot the normalized autocorrelation function for the lattice spacing, $\rho_a^{\mathrm{N6}}(t) = \Gamma_a^{\mathrm{N6}}(t)/\Gamma_a^{\mathrm{N6}}(0)$, and on the right accordingly for the quantity ϕ defined in eq. (2.15). For the lattice spacing data that enters ρ_a, measurements have been performed on each stored configuration, separated by 4 MDU, while for ϕ measurements are separated by 8 MDU.

different chiral and continuum extrapolations to the physical point $(m_\pi, a) = (m_\pi^{\mathrm{exp}}, 0)$. The latter are being discussed in more detail in Section 3. Finally, we collect the values of the static quantities $f_{\mathrm{B}}^{\mathrm{stat}}$, $f_{\mathrm{B_s}}^{\mathrm{stat}}$ and $f_{\mathrm{B_s}}^{\mathrm{stat}}/f_{\mathrm{B}}^{\mathrm{stat}}$ in Table 3.

2.4 Error analysis and propagation

We follow [41, 42] for all sources of errors. All results or intermediate quantities are considered as functions $f(\bar{p}, Y)$ of the means $\bar{p}_\alpha(e) = N_e^{-1}\sum_{m=1}^{N_e} p_\alpha^m(e)$ of primary MC data $p_\alpha^m(e)$ originating from configuration m of the ensemble number e (corresponding to e-id in Table 2 and 3), as well as functions of additional input Y, such as the HQET parameters ω_i. Also the results of fits to the data are considered as functions of the original data, where the weights in the fits (we always use only the diagonal errors as weights) are precomputed and then kept fixed, i.e., a dependence of f on the weights is not considered.

The error σ_f of such a function is then

$$\sigma_f^2 = \sum_e \sigma_f^2(e) + \sum_{i,j} \frac{\partial f}{\partial Y_i} C_{ij}^Y \frac{\partial f}{\partial Y_j} \,. \tag{2.18}$$

The block-diagonal covariance matrix C^Y of the additional input is known: a block [34] for the axial current renormalization factors at the three different β (entering the lattice spacing determination and f_π) and a block [30] for the ω_i. The contributions from the individual ensembles e are

$$\begin{aligned}\sigma_f^2(e) &= \frac{1}{N_e}\left[\Gamma_f^e(0) + 2\sum_{m=1}^{W-1}\Gamma_f^e(m) + 2\tau_{\mathrm{exp}}^e\Gamma_f^e(W)\right] \,, \\ \Gamma_f^e(m) &= \sum_{\alpha,\beta}\frac{\partial f}{\partial \bar{p}_\alpha}\Gamma_{\alpha\beta}^e(m)\frac{\partial f}{\partial \bar{p}_\beta} \,.\end{aligned} \tag{2.19}$$

The term proportional to τ_{exp}^e accounts for the difficult-to-estimate contribution of the tails to the autocorrelation function Γ_f^e [42]. For τ_{exp}^e we insert our previously estimated values

$\beta = 6/g_0^2$	$\kappa_{\rm crit}(g_0^2)$	$c_{\rm A}^{\rm stat}(g_0^2)$		$b_{\rm A}^{\rm stat}(g_0^2)$	
		HYP1	HYP2	HYP1	HYP2
5.2	0.1360546	0.0033461	0.0597692	0.6045384	0.6638461
5.3	0.1364572	0.0032830	0.0586415	0.6025660	0.6607547
5.5	0.1367749	0.0031636	0.0565090	0.5988363	0.6549090

Table 4: Numerical values of the improvement coefficients $b_{\rm A}^{\rm stat}$ and $c_{\rm A}^{\rm stat}$ from 1-loop PT [40].

(see e.g. Table 1 of [31]), and W is chosen as the point where Γ_f^e comes close to zero within about (1-2 $\times$) its estimated statistical error. The required derivatives $\frac{\partial f}{\partial \bar{p}_\alpha}$ are computed numerically [41].

We note that there are many hidden correlations which are all taken into account, e.g., the lattice spacing at one β depends on information from other β through the combined chiral extrapolation in [34]. A straightforward implementation of eq. (2.19) would be cumbersome and numerically expensive. We compute it iteratively instead [43, 44].

As explicit example we choose the ensemble with the highest statistics available, $e =$ N6. Figure 2 shows the numerical estimate of the normalized autocorrelation function $\rho(t)$ in terms of the simulation time in molecular dynamic units (MDU). After summing up the autocorrelation function explicitly within a window where it is still rather well determined, the sum up to infinity is determined by modelling it with a single exponential $\exp(-t/\tau_{\rm exp})$ plotted as "tail". On the left hand side of the figure the observable chosen is the lattice spacing (see [34]); the relevant contribution is from the kaon decay constant. On the right hand side we have chosen ϕ, i.e., essentially the B-meson decay constant in lattice units (see eq. (2.15)). While on the left, where only light-quark physics enters and measurements were taken more frequently, the tail is seen quite well at $t < 100$ MDU, on the right the autocorrelation function appears to drop to a lower value at short time and in fact is not significant at $t \approx 30$ MDU. Still, our somewhat conservative procedure estimates a $\approx 35\%$ contribution to $\tau_{\rm int}$ on the left and $\approx 82\%$ on the right.

3 Continuum and chiral limit extrapolations

We use formulae from Heavy Meson Chiral Perturbation Theory (HMχPT) when applicable [45–47]:

$$\begin{aligned}
\sqrt{\tfrac{m_{\rm B}}{2}}\, f_{\rm B}^{\delta}(y,a) &= A\left[1 - \tfrac{3}{4}\tfrac{1+3\widehat{g}^2}{2}\left\{y\log(y) - y^{\rm exp}\log(y^{\rm exp})\right\}\right] + C\,(y - y^{\rm exp}) + D^{\delta}\,a^2\ , \\
\sqrt{\tfrac{m_{\rm B_s}}{2}}\, f_{\rm B_s}^{\delta}(y,a) &= A_{\rm s} + C_{\rm s}\,(y - y^{\rm exp}) + D_{\rm s}^{\delta}\,a^2\ .
\end{aligned} \tag{3.1}$$

As in [31] we have parameterized the chiral behaviour through the variable $y = m_\pi^2/8\pi^2 f_\pi^2$, with $y^{\rm exp}$ representing the physical value at $f_\pi^{\rm exp} = 130.4\,$MeV and $m_\pi^{\rm exp} = 134.98\,$MeV. Since we employ two static discretizations, we also need to account for different cutoff effects, parameterized by D^δ, with $\delta = 1, 2$ corresponding to HYPδ. Due to the universality of the continuum limit, the other coefficients do not depend upon δ. After having fixed the HQET parameters at the physical b-quark mass, see Table 1, we treat the B-meson masses as constants, which are taken as $m_{\rm B} = 5279.5\,$MeV and $m_{\rm B_s} = 5366.3\,$MeV from the PDG [48]. Together with all data points that enter the joint chiral and continuum

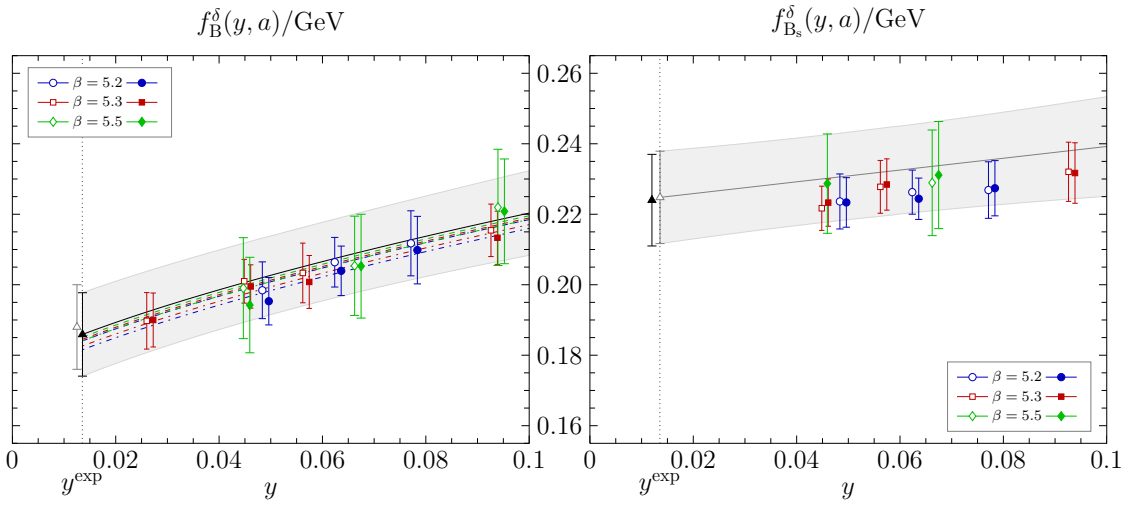

Figure 3: Extrapolation of the B (left panel) and B_s (right panel) meson decay constant to the physical point. On the left, the extrapolation using HMχPT at NLO (filled triangle) is compared to a linear one (open triangle), in order to extract the systematic error from truncating HMχPT at NLO. For $f_{\rm B_s}$ only a LO formula is known and shown. As a comparison we also add our final result, the continuum value of $f_{\rm B_s} = [f_{\rm B_s}/f_{\rm B}]f_{\rm B}$. All data points are listed in Table 2.

extrapolation, we list our results from different, independent fit ansätze in Table 2 and 3. For consistency, we decided to treat $f_{\rm B_s}$ as the dependent observable, to be derived from our final results

$$f_{\rm B} = 186(13)(2)_\chi\,{\rm MeV}\,, \qquad\qquad f_{\rm B_s}/f_{\rm B} = 1.203(62)(19)_\chi\,. \tag{3.2}$$

The first, statistical, error as obtained from the NLO HMχPT fit ansatz also includes the discrepancy to the static result, the uncertainty from the HQET parameters and the lattice spacings. We add a second, systematic, error to account for the uncertainty in the chiral extrapolation. It is given by the difference between the quoted value and its counterpart obtained by employing the LO fit ansatz for the chiral extrapolation. While we show only the NLO extrapolation of $f_{\rm B}$ in the left panel of Figure 3, we also add the continuum extrapolated value from the LO fit ansatz. With all correlations taken into account, our estimate for the $\rm B_s$-meson decay constant becomes

$$f_{\rm B_s} = 224(14)(2)_\chi\,{\rm MeV}\,. \tag{3.3}$$

In the right panel of Figure 3, we contrast this result (filled triangle) with an extrapolation of our $f_{\rm B_s}$ lattice data as if treated as an independent observable, c.f. Table 2. We have also tried a continuum extrapolation keeping a term linear in a in the fit functions. In fact, we have not included $\mathrm{O}(a)$ improvement terms in the HQET action and current insertions at $\mathrm{O}(1/m_{\rm h})$. These effects, formally of $\mathrm{O}(a/m_{\rm h})$, are expected to be small, and within our error we do not observe any such dependence.

To get an insight on the convergence in $1/m_{\rm h}$, it is interesting to compare our estimates at subleading order with those at static order of HQET. By applying the same fit formulae as in eqs. (3.1), we obtain

$$f_{\rm B}^{\rm stat} = 190(5)(2)_\chi\,{\rm MeV}\,, \qquad \frac{f_{\rm B_s}^{\rm stat}}{f_{\rm B}^{\rm stat}} = 1.189(24)(30)_\chi, \qquad f_{\rm B_s}^{\rm stat} = 226(6)(9)_\chi\,{\rm MeV}\,. \tag{3.4}$$

Source	$f_{\mathrm{B_s}}$	f_{B}	$f_{\mathrm{B_s}}/f_{\mathrm{B}}$	$f_{\mathrm{B_s}}^{\mathrm{stat}}$	$f_{\mathrm{B}}^{\mathrm{stat}}$	$f_{\mathrm{B_s}}^{\mathrm{stat}}/f_{\mathrm{B}}^{\mathrm{stat}}$
A3	0.20 %	0.19 %	0.00 %	1.22 %	1.10 %	0.00 %
A4	5.94 %	9.36 %	14.27 %	8.06 %	2.76 %	14.36 %
A5	1.17 %	6.51 %	7.37 %	2.01 %	0.91 %	3.10 %
B6	3.32 %	2.99 %	0.00 %	2.70 %	1.44 %	0.26 %
E5	1.15 %	1.28 %	0.21 %	1.00 %	0.95 %	0.01 %
F6	1.70 %	2.21 %	6.44 %	1.85 %	2.62 %	9.65 %
F7	15.41 %	5.79 %	37.01 %	14.89 %	3.02 %	40.32 %
G8	13.96 %	12.81 %	0.00 %	15.36 %	13.26 %	0.00 %
N5	5.91 %	5.43 %	0.00 %	9.17 %	7.94 %	0.00 %
N6	19.42 %	13.78 %	29.87 %	8.35 %	24.10 %	28.61 %
O7	16.03 %	25.46 %	4.80 %	19.91 %	27.66 %	3.58 %
ω	14.02 %	12.72 %	0.01 %	8.35 %	7.21 %	0.00 %
Z_{A}	1.77 %	1.46 %	0.01 %	7.13 %	7.04 %	0.09 %

Table 5: Distribution of relative squared errors among different sources for (3.2)–(3.4).

In Table 5 we split the statistical error of our observables among different sources. Obviously, the errors from the HQET parameters ω and renormalization factor Z_{A} which enters through the scale setting, largely cancel in the ratio. Although one looses precision, in general, due to the increased variance in HQET observables compared to observables in the light quark sector (such as m_π or f_π), one is in the fortunate position that the former couple less to the slow modes of the Monte Carlo chain, and therefore their integrated autocorrelation times are smaller than for "light" quantities.

3.1 A quick look at phenomenology

The Flavour Lattice Averaging Group (FLAG) [49] has made a selection of lattice results for f_{B}, $f_{\mathrm{B_s}}$ and $f_{\mathrm{B_s}}/f_{\mathrm{B}}$ with $N_{\mathrm{f}} = 2$, $2+1$ and $2+1+1$ dynamical quarks [17–22]. Only one determination entered the two-flavour average and has been updated [18] since. Their values $f_{\mathrm{B}} = 189(8)\,\mathrm{MeV}$, $f_{\mathrm{B_s}} = 228(8)$ and $f_{\mathrm{B_s}}/f_{\mathrm{B}} = 1.206(24)$ are fully compatible with ours. Averaging both $N_{\mathrm{f}} = 2$ results produces numbers which are consistent with the estimate from $N_{\mathrm{f}} = 2+1$ computations quoted by FLAG: $f_{\mathrm{B}}^{N_{\mathrm{f}}=2+1} = 190.5(4.2)\,\mathrm{MeV}$, $f_{\mathrm{B}}^{N_{\mathrm{f}}=2+1} = 227.7(4.5)$ and $f_{\mathrm{B_s}}/f_{\mathrm{B}} = 1.202(22)$.
As a phenomenological application, we can insert our results for f_{B} and $f_{\mathrm{B_s}}$ into the formulae describing the branching ratios of $B \to \tau\nu_\tau$ and $B_{\mathrm{s}} \to \mu^+\mu^-$ transitions:

$$\mathcal{B}(B^- \to \tau^-\bar{\nu}_\tau) = \frac{G_{\mathrm{F}}^2 |V_{\mathrm{ub}}|^2}{8\pi} \tau_{\mathrm{B}} f_{\mathrm{B}}^2 m_{\mathrm{B}} m_\tau^2 \times \left(1 - \frac{m_\tau^2}{m_{\mathrm{B}}^2}\right)^2 , \tag{3.5}$$

$$\mathcal{B}(B_{\mathrm{s}} \to \mu^+\mu^-) = \frac{G_{\mathrm{F}}^2}{\pi} \left[\frac{\alpha_{em}(m_Z)}{4\pi \sin^2\theta_{\mathrm{W}}}\right]^2 \tau_{\mathrm{B_s}} f_{\mathrm{B_s}}^2 m_{\mathrm{B_s}} m_\mu^2 \sqrt{1 - \frac{4m_\mu^2}{m_{\mathrm{B_s}}^2}}\, |V_{\mathrm{tb}}^* V_{\mathrm{ts}}|^2\, Y^2 .$$

Here $Y \equiv Y(x_{\mathrm{tW}}, x_{\mathrm{Ht}}, \alpha_s)$ takes into account various electroweak and QCD corrections, parameterized by $x_{\mathrm{tW}} = m_{\mathrm{t}}^2/m_{\mathrm{W}}^2$ and $x_{\mathrm{Ht}} = M_{\mathrm{H}}^2/m_{\mathrm{t}}^2$ with M_{H} being the Higgs boson mass. Using as inputs the experimental value $\mathcal{B}(B \to \tau\nu_\tau)_{\mathrm{exp}} = 1.05(25) \times 10^{-4}$ quoted by the PDG [2, 48, 50–52] and our estimate of f_{B}, we get

$$|V_{\mathrm{ub}}| = 4.15\,(29)_{f_{\mathrm{B}}}(48)_{\mathcal{B}} \times 10^{-3}, \tag{3.6}$$

where the errors come from $f_{\rm B}$ and the branching ratio, respectively. The value is roughly 1.5 σ above the exclusive determination from $B \to \pi\ell\nu$.

Moreover, using the recent combination of experimental measurements at LHC, namely $\mathcal{B}(B_{\rm s} \to \mu^+\mu^-) = (2.9 \pm 0.7) \times 10^{-9}$ [6,7,53], together with our determination of $f_{\rm B_s}$, and all input parameters of (3.5) set as in [8], we obtain

$$|V_{\rm tb}^* V_{\rm ts}| = 3.89\,(24)_{f_{\rm B_s}}(47)_{\mathcal{B}} \times 10^{-2}\,. \tag{3.7}$$

The number is in good agreement with the extraction from global fits, which is mostly constrained by $B_{\rm s}^0 - \overline{B_{\rm s}^0}$ mixing.

4 Conclusions

In this paper we have reported on our lattice measurement of the decay constants $f_{\rm B}$ and $f_{\rm B_s}$ performed with two dynamical flavours of O(a) improved Wilson fermions. The b-quark is treated in HQET, with the matching to QCD performed non-perturbatively. This makes the computation entirely non-perturbative, with no reference to continuum renormalized perturbation theory at any point. After an extrapolation to the chiral and continuum limit, we obtain

$$f_{\rm B} = 186(13)\,\text{MeV}\,, \qquad f_{\rm B_s}/f_{\rm B} = 1.203(65)\,, \qquad f_{\rm B_s} = 224(14)\text{MeV}\,. \tag{4.1}$$

Though it is important to check the dependence of these results on the number of dynamical flavours, and therefore to repeat the computation with a dynamical strange quark, it may still be interesting to compute the ratios $f_{\rm B^*}/f_{\rm B}$ and $f_{\rm B_0^*}/f_{\rm B}$ on the $N_{\rm f} = 2$ ensembles. The first one is often used to check the reliability of sum rules in the B-sector [54]. A lattice measurement at O($1/m_{\rm b}$) requires the matching coefficients that are being computed by the ALPHA Collaboration to extract $B \to \pi\ell\nu$ form factors [55]. The second ratio, already in the static limit, can be used to gain some insight into the precision of phenomenological applications of HMχPT, in particular concerning the relevance of the contributions from the $J^P = \{0^+,\, 1^+\}$ doublet states in chiral loops [56].

The method of the present paper to compute B-meson decay constants has been used previously in the framework of quenched QCD to estimate $f_{\rm B_s}$ without inclusion of virtual quark loops [33]. There, the scale r_0 defined via the static quark potential [57] was employed to express the decay constant in physical units, corresponding to $f_{\rm B_s}^{N_{\rm f}=0} = 216(5)\,\text{MeV}$ for $r_0 = 0.5\,\text{fm}$ and $f_{\rm B_s}^{N_{\rm f}=0} = 252(7)\,\text{MeV}$ for $r_0 = 0.45\,\text{fm}$. Given the rather reliable evidence that the true r_0 in physical units lies in between these values (see [58] for a review of the current status), our final result in eq. (4.1) is compatible with the quenched one at the present level of precision. Hence, no significant $N_{\rm f}$-dependence can be stated.

An interesting piece of information is also contained in the technical Table 5. It shows that the uncertainties in the non-perturbatively determined HQET parameters contribute only at the level of 8% in the static limit and 14% when $1/m_{\rm b}$ terms are included. Moreover, we find the O($1/m_{\rm b}$) corrections to be very small, $\lesssim 2.5\%$. This, together with the fact that the computation of the ω_i can be much improved with today's machines, gives us confidence that errors can be significantly reduced in the future computation with 2+1 dynamical flavours.

Acknowledgements. We would like to thank S. Lottini for many helpful discussions as well as for providing us with the latest results on f_π, m_π and f_K prior to their final publication. Furthermore, we appreciate the support of many colleagues within the CLS effort for the joint production and use of gauge configurations. This work is supported in part by the SFB/TR 9, by grant HE 4517/2-1 (P.F. and J.H.) and HE 4517/3-1 (J.H.) of the Deutsche Forschungsgemeinschaft, and by the European Community through EU Contract MRTN-CT-2006-035482, "FLAVIAnet". It was also partially supported by the Spanish Ministry of Education and Science projects RyC-2011-08557 (M.D.M.). We gratefully acknowledge the computer resources granted by the John von Neumann Institute for Computing (NIC) and provided on the supercomputer JUROPA at Jülich Supercomputing Centre (JSC) and by the Gauss Centre for Supercomputing (GCS) through the NIC on the GCS share of the supercomputer JUQUEEN at JSC, with funding by the German Federal Ministry of Education and Research (BMBF) and the German State Ministries for Research of Baden-Württemberg (MWK), Bayern (StMWFK) and Nordrhein-Westfalen (MIWF), as well as within the Distributed European Computing Initiative by the PRACE-2IP, with funding from the European Community's Seventh Framework Programme (FP7/2007-2013) under grant agreement RI-283493, by the Grand Équipement National de Calcul Intensif at CINES in Montpellier under the allocation 2012-056808, by the HLRN in Berlin, and by NIC at DESY, Zeuthen.

References

[1] **BaBar** Collaboration, J. Lees et al., *Evidence of $B \to \tau\nu$ decays with hadronic B tags*, *Phys.Rev.* **D88** (2013) 031102, [arXiv:1207.0698].

[2] **Belle** Collaboration, I. Adachi et al., *Measurement of $B^- \to \tau^- \bar{\nu}_\tau$ with a Hadronic Tagging Method Using the Full Data Sample of Belle*, *Phys.Rev.Lett.* **110** (2013) 131801, [arXiv:1208.4678].

[3] **BaBar** Collaboration, P. del Amo Sanchez et al., *Measurement of the $B^0 \to \pi^- \ell^+ \nu$ and $B^+ \to \eta^{(\prime)} \ell^+ \nu$ Branching Fractions, the $B^0 \to \pi^- \ell^+ \nu$ and $B^+ \to \eta \ell^+ \nu$ Form-Factor Shapes, and Determination of $|V_{ub}|$*, *Phys.Rev.* **D83** (2011) 052011, [arXiv:1010.0987].

[4] **BELLE** Collaboration, H. Ha et al., *Measurement of the decay $B^0 \to \pi^- \ell^+ \nu$ and determination of $|V_{ub}|$*, *Phys.Rev.* **D83** (2011) 071101, [arXiv:1012.0090].

[5] W.-S. Hou, *Enhanced charged Higgs boson effects in $B^- \to \tau\bar{\nu}, \mu\bar{\nu}$ and $b \to \tau\bar{\nu} + X$*, *Phys.Rev.* **D48** (1993) 2342–2344.

[6] **LHCb** Collaboration, R. Aaij et al., *Measurement of the $B_s^0 \to \mu^+\mu^-$ branching fraction and search for $B^0 \to \mu^+\mu^-$ decays at the LHCb experiment*, *Phys.Rev.Lett.* **111** (2013) 101805, [arXiv:1307.5024].

[7] **CMS** Collaboration, S. Chatrchyan et al., *Measurement of the $B_s^0 \to \mu^+\mu^-$ branching fraction and search for $B^0 \to \mu^+\mu^-$ with the CMS Experiment*, *Phys.Rev.Lett.* **111** (2013) 101804, [arXiv:1307.5025].

[8] A. J. Buras, J. Girrbach, D. Guadagnoli, and G. Isidori, *On the Standard Model prediction for $\mathcal{B}(B_{s,d} \to \mu^+\mu^-)$*, *Eur.Phys.J.* **C72** (2012) 2172, [arXiv:1208.0934].

[9] A. J. Buras, R. Fleischer, J. Girrbach, and R. Knegjens, *Probing New Physics with the $B_s \to \mu^+\mu^-$ Time-Dependent Rate*, *JHEP* **1307** (2013) 77, [arXiv:1303.3820].

[10] V. Morénas, A. Le Yaouanc, L. Oliver, O. Pène, and J. Raynal, *Decay constants in the heavy quark limit in models à la Bakamjian and Thomas*, *Phys.Rev.* **D58** (1998) 114019, [hep-ph/9710298].

[11] D. Ebert, R. Faustov, and V. Galkin, *Relativistic treatment of the decay constants of light and heavy mesons*, *Phys.Lett.* **B635** (2006) 93–99, [hep-ph/0602110].

[12] A. Badalian, B. Bakker, and Y. Simonov, *Decay constants of the heavy-light mesons from the field correlator method*, *Phys.Rev.* **D75** (2007) 116001, [hep-ph/0702157].

[13] M. Jamin and B. O. Lange, *f_B and f_{B_s} from QCD sum rules*, *Phys.Rev.* **D65** (2002) 056005, [hep-ph/0108135].

[14] W. Lucha, D. Melikhov, and S. Simula, *Decay constants of heavy pseudoscalar mesons from QCD sum rules*, *J.Phys.* **G38** (2011) 105002, [arXiv:1008.2698].

[15] S. Narison, *Revisiting f_B and $m_b(m_b)$ from HQET spectral sum rules*, *Phys.Lett.* **B721** (2013) 269–276, [arXiv:1212.5544].

[16] M. J. Baker, J. Bordes, C. A. Dominguez, J. Peñarrocha, and K. Schilcher, *B Meson Decay Constants f_{B_c}, f_{B_s} and f_B from QCD Sum Rules*, arXiv:1310.0941.

[17] **ETM** Collaboration, P. Dimopoulos et al., *Lattice QCD determination of m_b, f_B and f_{B_s} with twisted mass Wilson fermions*, *JHEP* **1201** (2012) 046, [arXiv:1107.1441].

[18] **ETM** Collaboration, N. Carrasco et al., *B-physics from $N_f = 2$ tmQCD: the Standard Model and beyond*, *JHEP* **1403** (2014) 016, [arXiv:1308.1851].

[19] C. McNeile, C. Davies, E. Follana, K. Hornbostel, and G. Lepage, *High-Precision f_{B_s} and HQET from Relativistic Lattice QCD*, *Phys.Rev.* **D85** (2012) 031503, [arXiv:1110.4510].

[20] **Fermilab Lattice & MILC** Collaboration, A. Bazavov et al., *B- and D-meson decay constants from three-flavor lattice QCD*, *Phys.Rev.* **D85** (2012) 114506, [arXiv:1112.3051].

[21] H. Na et al., *The B and B_s Meson Decay Constants from Lattice QCD*, *Phys.Rev.* **D86** (2012) 034506, [arXiv:1202.4914].

[22] **HPQCD** Collaboration, R. Dowdall, C. Davies, R. Horgan, C. Monahan, and J. Shigemitsu, *B-meson decay constants from improved lattice NRQCD and physical u, d, s and c sea quarks*, *Phys.Rev.Lett.* **110** (2013) 222003, [arXiv:1302.2644].

[23] E. Eichten and B. Hill, *An effective field theory for the calculation of matrix elements involving heavy quarks*, *Phys. Lett.* **B234** (1990) 511.

[24] N. Isgur and M. B. Wise, *Weak decays in the static quark approximation*, *Phys. Lett.* **B232** (1989) 113–117.

[25] H. Georgi, *An effective field theory for heavy quarks at low energies*, *Phys. Lett.* **B240** (1990) 447–450.

[26] E. Eichten and B. R. Hill, *Static Effective Field Theory: $1/m$ Corrections*, *Phys.Lett.* **B243** (1990) 427–431.

[27] **ALPHA** Collaboration, J. Heitger and R. Sommer, *Non-perturbative heavy quark effective theory*, *JHEP* **02** (2004) 022, [hep-lat/0310035].

[28] **ALPHA** Collaboration, M. Della Morte, N. Garron, M. Papinutto, and R. Sommer, *Heavy quark effective theory computation of the mass of the bottom quark*, *JHEP* **01** (2007) 007, [hep-ph/0609294].

[29] **ALPHA** Collaboration, B. Blossier, M. Della Morte, N. Garron, and R. Sommer, *HQET at order $1/m$: I. Non-perturbative parameters in the quenched approximation*, *JHEP* **1006** (2010) 002, [arXiv:1001.4783].

[30] **ALPHA** Collaboration, B. Blossier et al., *Parameters of Heavy Quark Effective Theory from $N_f = 2$ lattice QCD*, *JHEP* **1209** (2012) 132, [arXiv:1203.6516].

[31] **ALPHA** Collaboration, F. Bernardoni et al., *The b-quark mass from non-perturbative $N_f = 2$ Heavy Quark Effective Theory at $O(1/m_h)$*, *Phys.Lett.* **B730** (2014) 171–176, [arXiv:1311.5498].

[32] R. Sommer, *Non-perturbative renormalization of HQET and QCD*, hep-lat/0209162.

[33] **ALPHA** Collaboration, B. Blossier et al., *HQET at order 1/m: III. Decay constants in the quenched approximation*, *JHEP* **1012** (2010) 039, [arXiv:1006.5816].

[34] **ALPHA** Collaboration, P. Fritzsch et al., *The strange quark mass and Lambda parameter of two flavor QCD*, *Nucl.Phys.* **B865** (2012) 397–429, [arXiv:1205.5380].

[35] **ALPHA** Collaboration, B. Blossier, M. Della Morte, G. von Hippel, T. Mendes, and R. Sommer, *On the generalized eigenvalue method for energies and matrix elements in lattice field theory*, *JHEP* **0904** (2009) 094, [arXiv:0902.1265].

[36] S. Güsken et al., *Nonsinglet axial vector couplings of the baryon octet in lattice QCD*, *Phys. Lett.* **B227** (1989) 266.

[37] **APE** Collaboration, M. Albanese et al., *Glueball masses and string tension in lattice QCD*, *Phys. Lett.* **192B** (1987) 163.

[38] S. Basak et al., *Combining Quark and Link Smearing to Improve Extended Baryon Operators*, *PoS* **LAT2005** (2006) 076, [hep-lat/0509179].

[39] **ALPHA** Collaboration, B. Blossier et al., *HQET at order $1/m$: II. Spectroscopy in the quenched approximation*, *JHEP* **1005** (2010) 074, [arXiv:1004.2661].

[40] A. Grimbach, D. Guazzini, F. Knechtli, and F. Palombi, *O(a) improvement of the HYP static axial and vector currents at one-loop order of perturbation theory*, *JHEP* **0803** (2008) 039, [arXiv:0802.0862].

[41] **ALPHA** Collaboration, U. Wolff, *Monte Carlo errors with less errors*, *Comput.Phys.Commun.* **156** (2004) 143–153, [hep-lat/0306017].

[42] **ALPHA** Collaboration, S. Schaefer, R. Sommer, and F. Virotta, *Critical slowing down and error analysis in lattice QCD simulations*, *Nucl.Phys.* **B845** (2011) 93–119, [arXiv:1009.5228].

[43] **ALPHA** Collaboration, H. Simma, R. Sommer, and F. Virotta, *General error computation in lattice gauge theory*, . Internal notes of the ALPHA collaboration (2014).

[44] S. Lottini and R. Sommer, *Data analysis in lattice field theory*, Lattice practices, DESY, Zeuthen (2014). https://indico.desy.de/conferenceDisplay.py?confId=9420.

[45] J. Goity, *Chiral perturbation theory for SU(3) breaking in heavy meson systems*, *Phys.Rev.* **D46** (1992) 3929–3936, [hep-ph/9206230].

[46] S. R. Sharpe and Y. Zhang, *Quenched chiral perturbation theory for heavy-light mesons*, *Phys.Rev.* **D53** (1996) 5125–5135, [hep-lat/9510037].

[47] F. Bernardoni, P. Hernandez, and S. Necco, *Heavy-light mesons in the ϵ-regime*, *JHEP* **1001** (2010) 070, [arXiv:0910.2537].

[48] **Particle Data Group** Collaboration, J. Beringer et al., *Review of Particle Physics (RPP)*, *Phys.Rev.* **D86** (2012) 010001.

[49] S. Aoki et al., *Review of lattice results concerning low energy particle physics*, arXiv:1310.8555.

[50] **BaBar** Collaboration, B. Aubert et al., *A Search for $B^+ \to \tau^+\nu$ with Hadronic B tags*, *Phys.Rev.* **D77** (2008) 011107, [arXiv:0708.2260].

[51] **BaBar** Collaboration, B. Aubert et al., *A Search for $B^+ \to \ell^+\nu_\ell$ Recoiling Against $B^- \to D^0\ell^-\bar{\nu}X$*, *Phys.Rev.* **D81** (2010) 051101, [arXiv:0912.2453].

[52] **Belle** Collaboration, K. Hara et al., *Evidence for $B^- \to \tau^- \bar{\nu}$ with a Semileptonic Tagging Method*, *Phys.Rev.* **D82** (2010) 071101, [arXiv:1006.4201].

[53] **CMS and LHCb** Collaboration, *Combination of results on the rare decays $B^0_{(s)} \to \mu^+\mu^-$ from the CMS and LHCb experiments*, Tech. Rep. CMS-PAS-BPH-13-007. CERN-LHCb-CONF-2013-012, CERN, Geneva, Jul, 2013. http://cds.cern.ch/record/1564324.

[54] S. Bekavac et al., *Matching QCD and HQET heavy-light currents at three loops*, *Nucl.Phys.* **B833** (2010) 46–63, [arXiv:0911.3356].

[55] **ALPHA** Collaboration, M. Della Morte, S. Dooling, J. Heitger, D. Hesse, and H. Simma, *Matching of heavy-light flavour currents between HQET at order 1/m and QCD: I. Strategy and tree-level study*, arXiv:1312.1566.

[56] D. Bećirević, S. Fajfer, and S. Prelovšek, *On the mass differences between the scalar and pseudoscalar heavy-light mesons*, *Phys.Lett.* **B599** (2004) 55, [hep-ph/0406296].

[57] R. Sommer, *A New way to set the energy scale in lattice gauge theories and its applications to the static force and α_s in SU(2) Yang-Mills theory*, *Nucl.Phys.* **B411** (1994) 839–854, [hep-lat/9310022].

[58] R. Sommer, *Scale setting in lattice QCD*, arXiv:1401.3270.